

Supplementary Material

Mo-doped ZnO NPs with NIR light enhanced peroxidase-like nanozyme as photocatalytic and antimicrobial applications

Yini Xu ^{a#}, Jinya Wei ^{b#}, Dezhi Yang, Yuzhu Song ^{a*}, Yaling Yang ^{a*}

^a Faculty of Life Science and Technology, Kunming University of Science and Technology, Kunming 650500, People's Republic of China.

^b Yunnan High-tech Enterprise Development Promotion Association, Kunming 650021, People's Republic of China.

*Corresponding author: Yaling Yang, E-mail: 13313116@kust.edu.cn; Yuzhu Song, E-mail: yuzhusong@kust.edu.cn

1. Materials

Sodium molybdate ($\text{Na}_2\text{MoO}_4 \cdot 7\text{H}_2\text{O}$), zinc nitrate ($\text{ZnNO}_3 \cdot 6\text{H}_2\text{O}$), Sodium hydroxide (NaOH), Acetic acid and Sodium acetate were obtained from Tianjin Zhiyuan Reagent Co. Ltd. Hexamethylene tetramine was obtained from Guangzhou Pharmaceuticals Co. Ltd. 3,3',5,5'-Tetramethylbenzidine (TMB) 3,3',5,5'-Tetramethylbenzidine (TMB) were purchased from Tianjin Hiens Biochemical Technology Co., Ltd. Ethanol, hydrogen peroxide (H_2O_2 , 30 wt%) was bought from Sigma-Aldrich (Shanghai, China). *Staphylococcus aureus* (*S. aureus*, ATCC-6538), *Escherichia coli* (*E. coli*, ATCC-8099), Ampicillin-resistant *Escherichia coli* (AREC, SHBCC D25148) and Methicillin-resistant *Staphylococcus aureus* (MRSA, ATCC 43300) were received from Shanghai Bioresource Collection Center. All aqueous solutions used in the experiments were prepared with deionized water (18.2 MΩ ·cm, Millipore).

2. Characterization

Using a 200 kV accelerating voltage, the TecnaiG2 TF20 transmission electron microscopy (TEM) was used to examine the morphology and microstructure of the Mo/ZnO NPs. Thermo Scientific K-Alpha Nexsa X-ray photoelectron spectroscopy (XPS) fitted with Al X-ray source analysis was used to examine the molecular states of the Mo/ZnO NPs. Additional verification of its composition was conducted using a Bruker Tensor 27 spectrometer that was connected to the Hyperion microscope. The spectrometer had an MCT (HgCdTe) detector that was cooled using liquid nitrogen. Using a Beijing General Analysis Instrument Co. Ltd. TU-1901 Double beam UV-visible spectrophotometer, UV-vis absorption spectra were measured.

Figures:

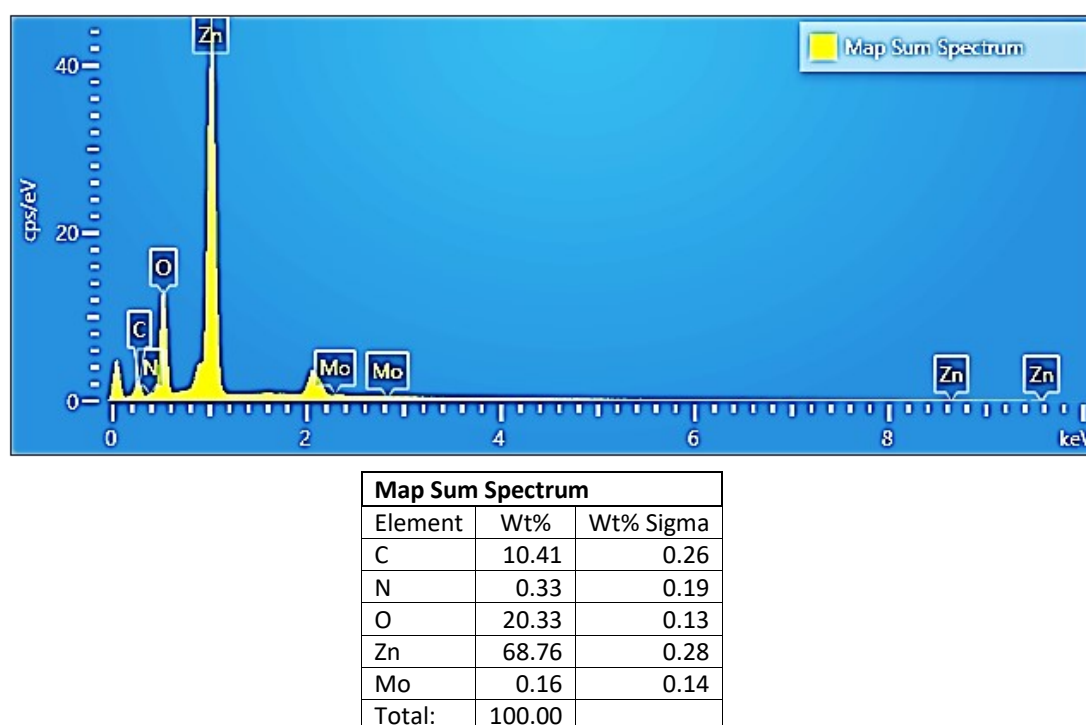


Fig. S1 The EDS spectrum of the Mo/ZnO NPs microstructures.

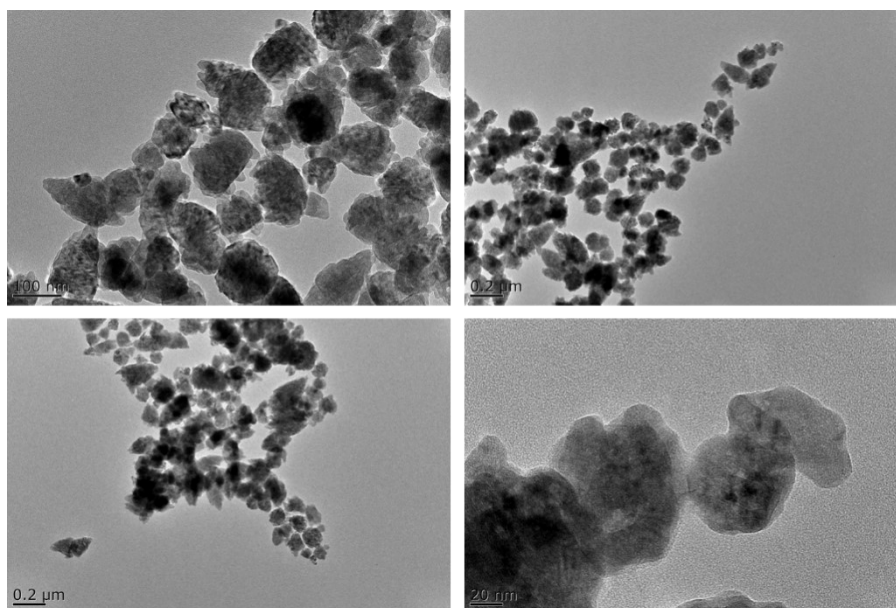


Fig. S2 TEM image of Mo/ZnO

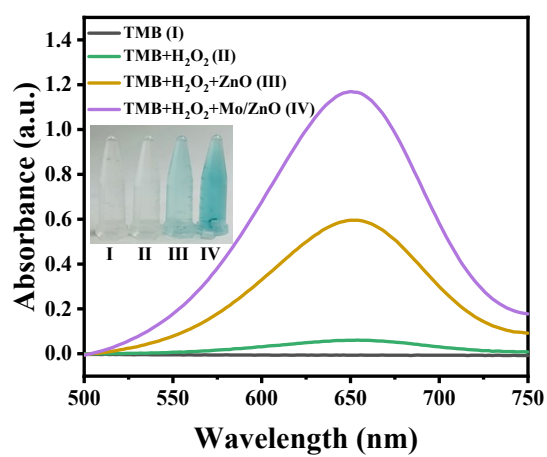
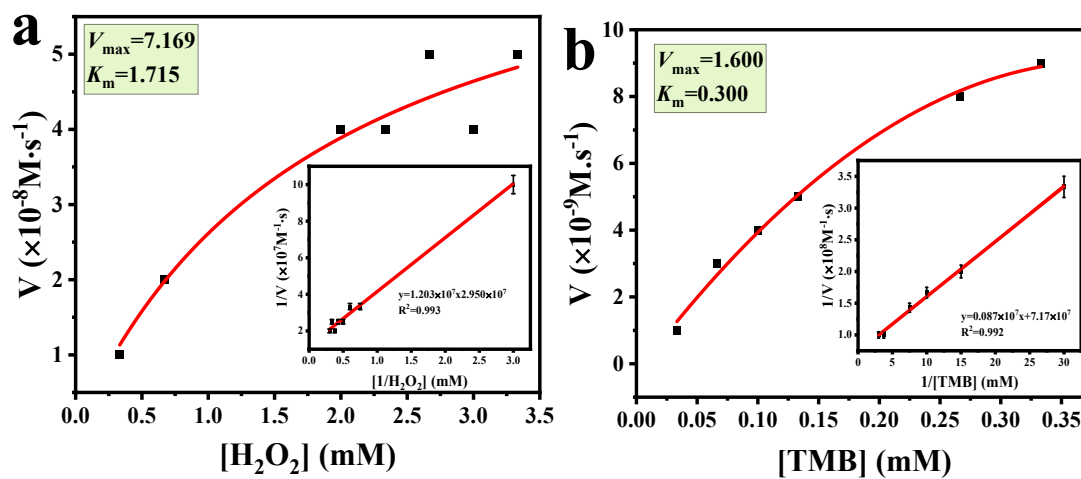


Fig.S3 Comparison of POD-like activity of ZnO and ZnO@Mo



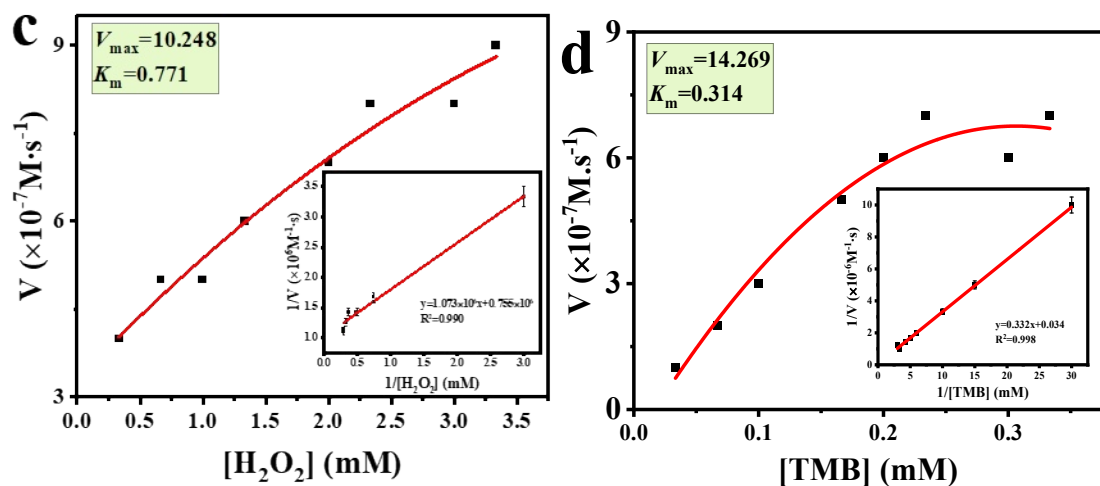


Fig. S4 Steady-state kinetic analysis of Mo/ZnO NPs (a) H_2O_2 , (b) TMB; Mo/ZnO NPs (c) H_2O_2 +NIR, (d) TMB+NIR;

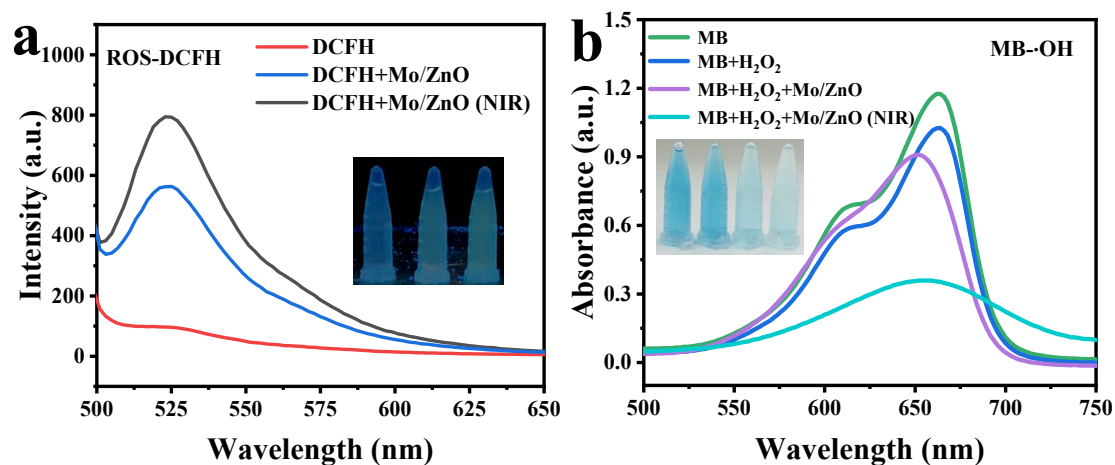


Fig. S5 (a)The DCFH validation of ROS. (b) The MB validation of $\cdot\text{OH}$.

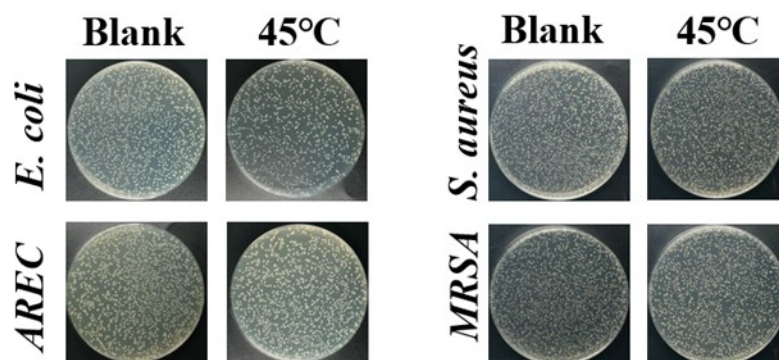


Fig. S6 The influence of temperature on *E. coli*, AREC, *S. aureus* and MRSA.

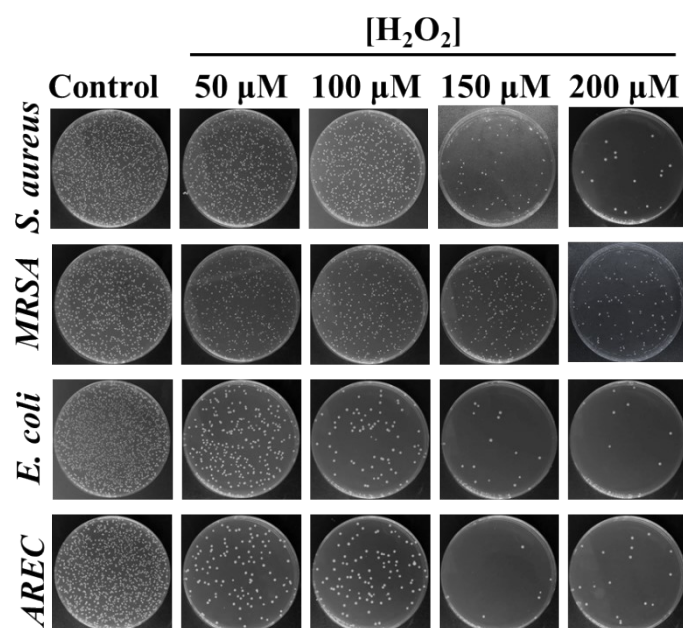
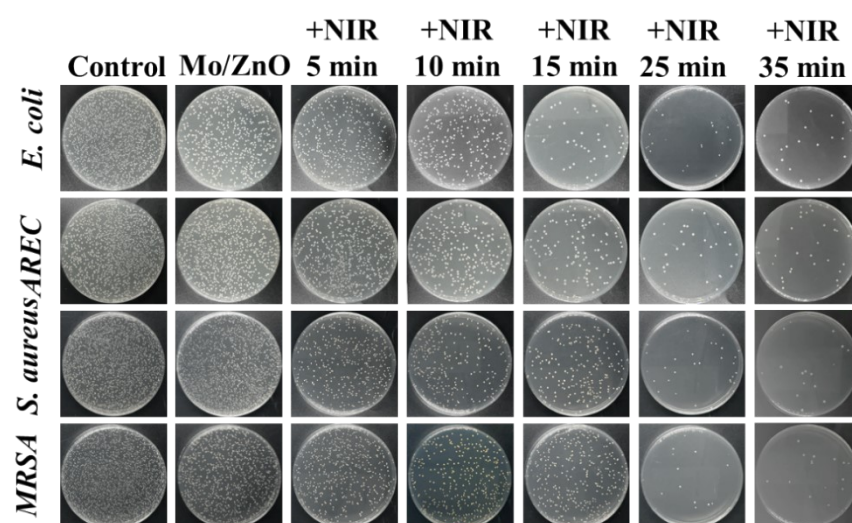


Fig. S7 The effect of H_2O_2 concentration on the antibacterial activity of Mo/ZnO NPs.



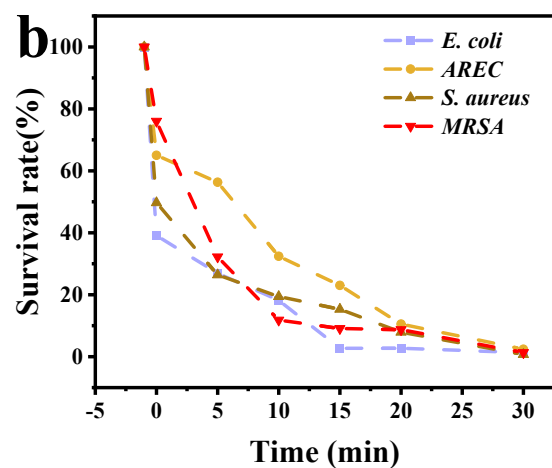
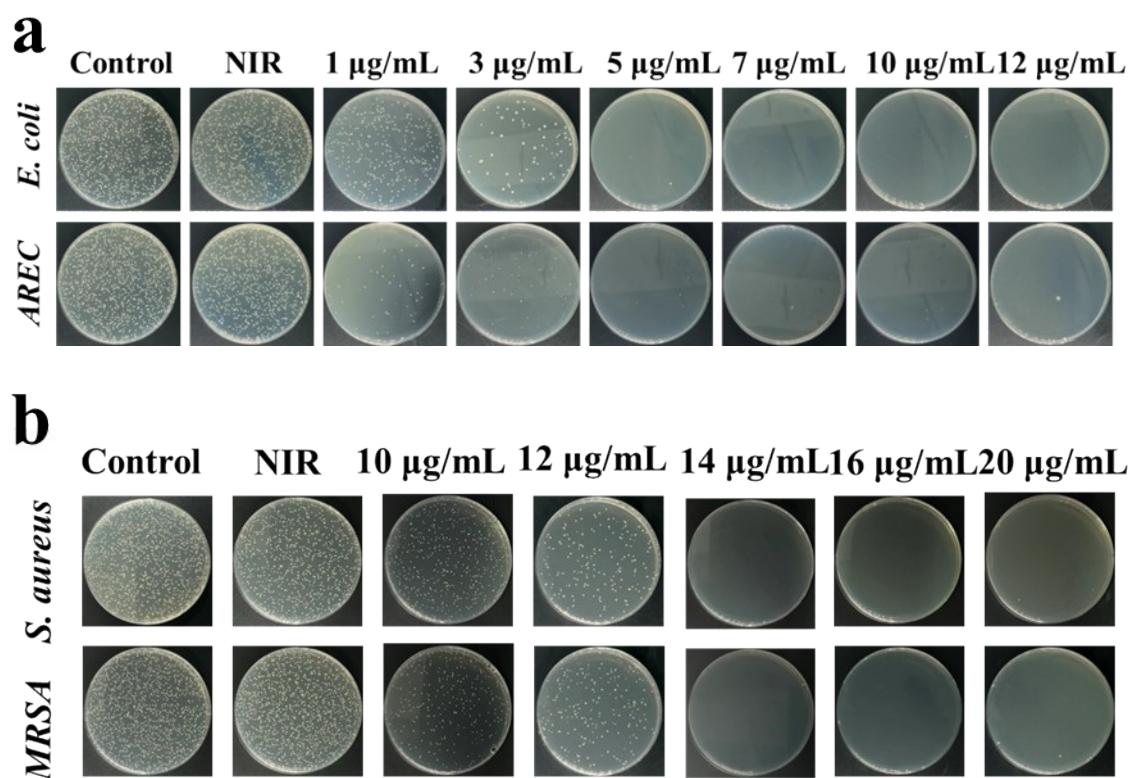


Fig. S8 The effect of reaction time on the antibacterial activity of Mo/ZnO NPs.



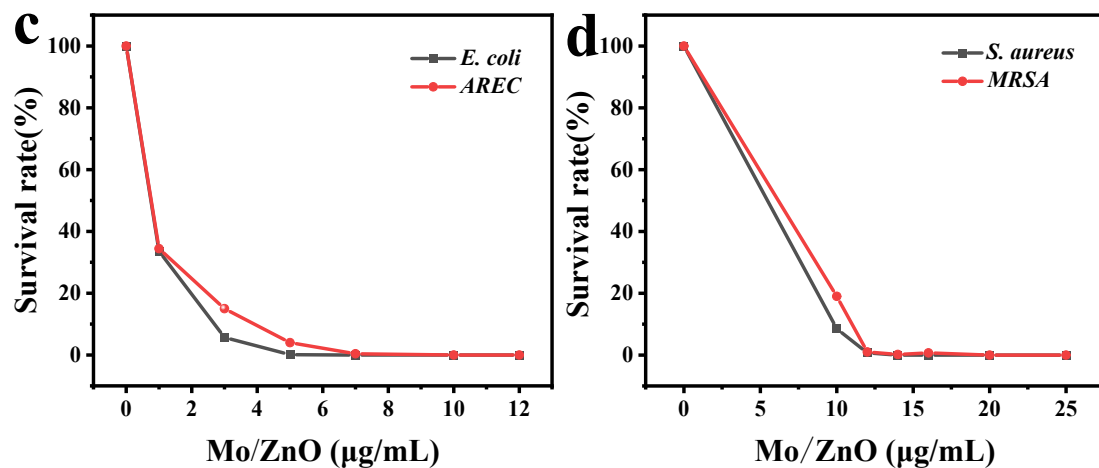


Fig. S9 Effect of antimicrobial activity of Mo/ZnO NPs concentration.

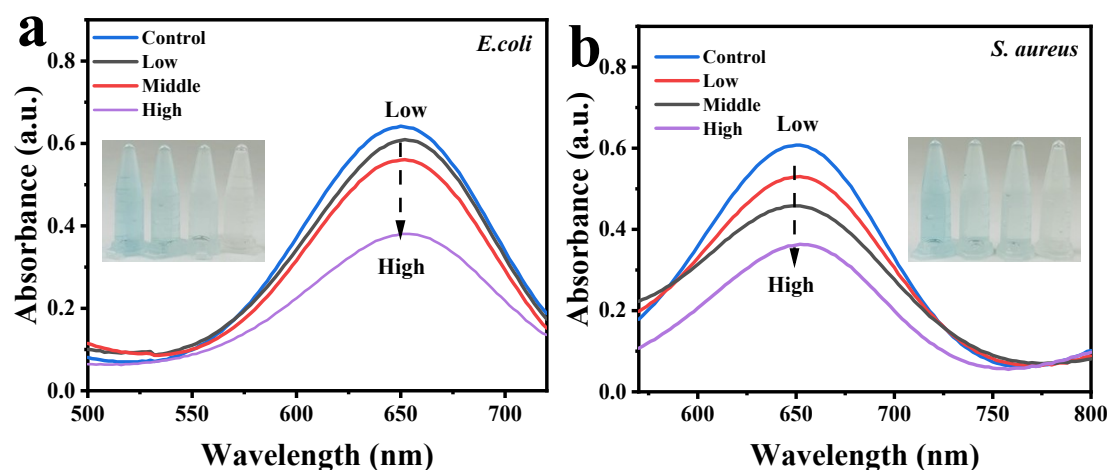


Fig. S10 ROS generated by Mo/ZnO NPs and the H_2O_2 system are absorbed by bacteria.

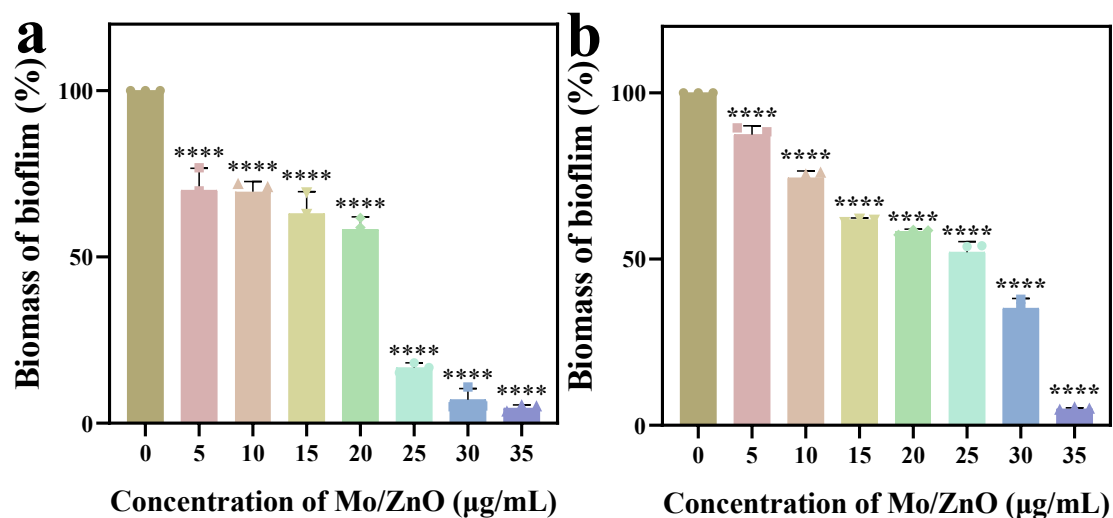


Fig. S11 Performance of Mo/ZnO NPs in inhibiting biofilm production by AREC,

MRSA.

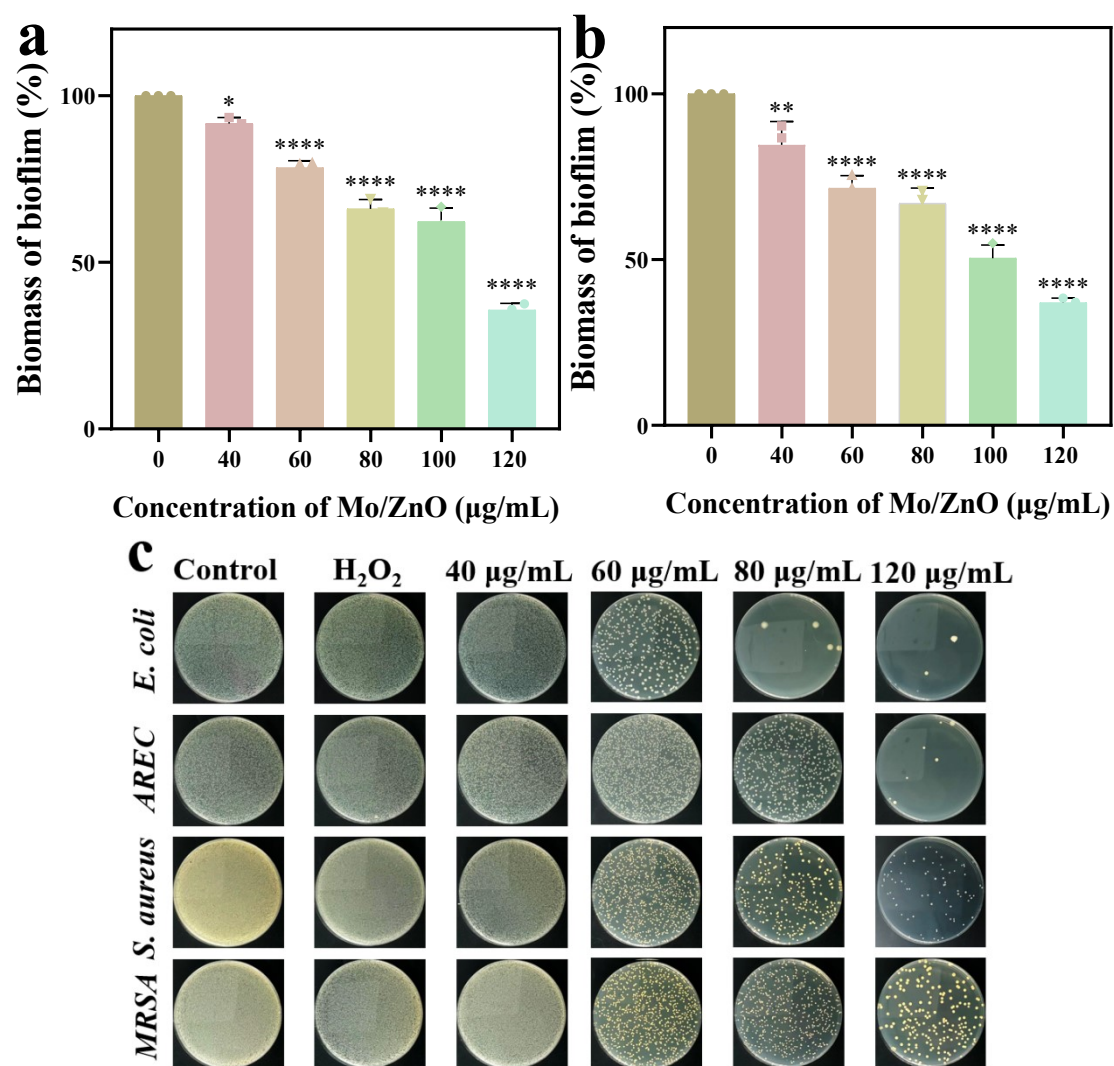


Fig. S12 (a-b) Performance of Mo/ZnO NPs in eliminating mature biofilms of AREC, MRSA. (c) The formed biofilm was beaten into PBS and mixed well before coating the plate.

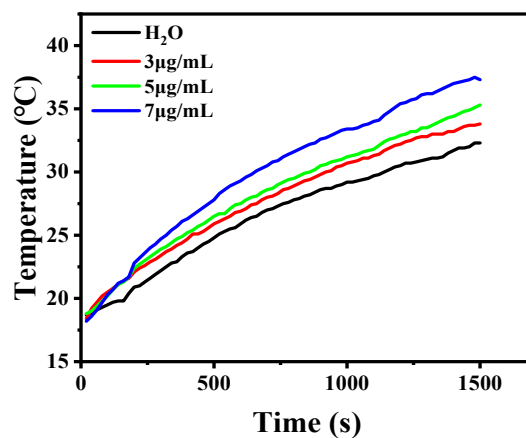


Fig. S13 Temperature elevation curves of Mo/ZnO NPs at the different concentrations
irradiated by 808 nm laser